HHS Public Access

Author manuscript

*Nat Struct Mol Biol*. Author manuscript; available in PMC 2012 June 20.

Published in final edited form as:

*Nat Struct Mol Biol*. 2011 April ; 18(4): 504–506. doi:10.1038/nsmb.2035.

# Structural organization of brain-derived mammalian prions as probed by hydrogen exchange

**Vytautas Smirnovas**[1,3], **Gerald S. Baron**[2,3], **Danielle K. Offerdahl**[2], **Gregory J. Raymond**[2], **Byron Caughey**[2], and **Witold K. Surewicz**[1,*]

[1]Department of Physiology and Biophysics, Case Western Reserve University, Cleveland, OH 44106

[2]Laboratory of Persistent Viral Diseases, Rocky Mountain Laboratories, National Institute of Allergy and Infectious Diseases, NIH, Hamilton, MT 59840

## Abstract

One of the mysteries in prion research is the structure of the infectious form of mammalian prion protein, $PrP^{Sc}$. We used MS analysis of H/D exchange to examine brain-derived $PrP^{Sc}$. Our data indicate that, contrary to popular models, prion protein conversion involves refolding of the entire region C-terminal to residue ~80–90, and that this region in $PrP^{Sc}$ consists of ß-strands and relatively short turns/loops, with no native α-helices present.

Transmissible spongiform encephalopathies (TSEs), or prion diseases, are a group of fatal neurodegenerative diseases including Creutzfeldt-Jakob disease in humans and bovine spongiform encephalopathy in cattle. These disorders are associated with conformational conversion of the normally monomeric and α-helical prion protein, $PrP^{C}$, to a misfolded aggregated form, $PrP^{Sc}$ (refs. 1,2). It is believed that $PrP^{Sc}$ itself represents the infectious prion agent, and this 'protein-only' model of TSE infectivity is supported by rapidly growing experimental data[1–6].

While the structure of $PrP^{C}$ is well characterized[7], a critical gap in the TSE field is the limited information regarding the structure of the rogue $PrP^{Sc}$ conformer. In fact, little specific structural information is available for $PrP^{Sc}$ aggregates beyond evidence of partial resistance to proteinase K digestion (with the PK-resistant core associated with prion infectivity usually starting at residue ~80–90 and extending to the C-terminus), and low-resolution spectroscopic data indicating that the $PrP^{C}\rightarrow PrP^{Sc}$ conversion is accompanied by



*Correspondence should be addressed to W.K.S. (witold.surewicz@case.edu).

[3]These authors contributed equally to this study

AUTHOR CONTRIBUTIONS

V.S performed and analyzed H/D exchange experiments. G.J.R. and D.K.O. performed all animal-associated work from animal inoculations to dissection of brain tissue. G.S.B., D.K.O. and G.J.R prepared $PrP^{Sc}$ samples and performed their biochemical characterization. B.C. performed FTIR experiments. W.K.S. wrote the manuscript and coordinated the entire project. G.S.B., V.S. and B.C. discussed the results and revised the manuscript.

COMPETING FINANCIAL INTERESTS

The authors declare no competing financial interests.

a substantial increase in ß-sheet structure[1,2,8–10]. Neither the part of the protein involved in this conformational transition nor the specific structural features responsible for high PK resistance are clear. In the absence of experimental data, current discussions regarding $PrP^{Sc}$ structure revolve around divergent theoretical models (see below).

While a number of approaches have recently emerged to probe the structure of ordered protein aggregates, most of them require the introduction of specific spectroscopic probes; therefore, they are not applicable to proteins derived from mammalian tissue. One of very few exceptions is H/D exchange coupled with mass spectrometry (HXMS). The H/D exchange method exploits the rapid exchange of backbone amide hydrogens within the unstructured regions of proteins compared to relatively slow exchange of those involved in systematically H-bonded structures such as ß-sheets or α-helices. These exchange rates are especially slow for amide protons in ‘ß-core’ regions of ordered aggregates such as amyloid fibrils[11]. Recently we used the HXMS approach to map the ß-sheet core in fibrils generated from recombinant human PrP[12]. Here we extend these studies to a much more challenging and biologically important system of authentic, mice brain-derived $PrP^{Sc}$.

The focus of our initial experiments was a structural characterization of the PK-resistant domain of $PrP^{Sc}$ purified from wild-type mice infected with 22L strain of mouse prions (WT 22L $PrP^{Sc}$). A prerequisite of HXMS analysis is the generation and identification of peptic fragments that can be rapidly separated by HPLC under the ‘exchange quenching’ conditions (see Supplementary Methods). For WT 22L $PrP^{Sc}$, we were able to identify 10 peptic fragments that fully cover the entire N-terminal part of the PK-resistant domain between residues 81 and 167. Remarkably, a very strong protection against deuterium labeling was observed for this entire region, with less than ~40 % deuterium incorporation after 240 hours of incubation in $D_2O$ (Fig. 1a). As discussed below, this high level of protection against deuterium incorporation indicates that the entire 81–167 region is involved in a highly ordered, systematically H-bonded ß-core of $PrP^{Sc}$ aggregates. In contrast to very good coverage for the 81–167 segment, only one peptic fragment could be identified for the C-terminal part of the protein, precluding H/D exchange studies for the latter region of $PrP^{Sc}$. This is largely caused by the presence of posttranslational modifications in wild-type prion protein (N-glycosylation at residues 180 and 196; GPI anchor at residue 230), as these modifications prevent identification of modified peptic fragments and/or interfere with peptic digestion itself.

To overcome this problem, we took advantage of recent findings regarding prion propagation in transgenic mice expressing GPI-free ($GPI^-$), largely unglycosylated $PrP^C$ (ref. 13). Upon inoculation with wild-type prions, these transgenic mice produce substantial quantities of $PrP^{Sc}$, and this material is highly infectious in second-passage experiments to wild-type mice[13]. To facilitate structural studies, PK-resistant $PrP^{Sc}$ was purified from brain tissue of $GPI^-$ PrP Tg mice infected with 22L, Chandler, or ME7 scrapie strains, yielding protein with purity better than ~90% as assessed by SDS PAGE (Supplementary Fig. 1).

For $GPI^-$ 22L $PrP^{Sc}$ we were able to identify 28 peptic fragments which give rise to mass spectra with a signal-to-noise ratio sufficient for reliable analysis of deuterium incorporation. These fragments cover ~90% of the sequence of the PK-resistant domain of

$PrP^{Sc}$, with multiple overlaps in some regions; the only gaps are for residues 168–181 and 213–216. This coverage represents a major improvement compared to that attainable for WT $PrP^{Sc}$, allowing more complete structural characterization.

The extent of deuterium incorporation for peptic fragments derived from $GPI^{-}$22L $PrP^{Sc}$ after 5 min and 240 h of isotope exchange is shown in Fig. 1b. Akin to WT 22L $PrP^{Sc}$, a high degree of protection against deuterium incorporation was observed for all peptic fragments derived from the 81–167 region, suggesting generally similar structural organization of WT and $GPI^{-}$ prions. Importantly, 240 h exchange data for $GPI^{-}$ 22L $PrP^{Sc}$ reveal that this highly exchange-protected structure extends almost to the C-terminus. Based on the level of deuterium incorporation by peptic fragment 224–231 (~65%), one can estimate the boundary of this protected domain around residue 226. The regions that show particularly strong resistance to H/D exchange (less than ~12% of deuterium labeling within 240 hours) include residues 127–132, ~149–167, 197–212 and 217–223. Backbone amides that undergo rapid H/D exchange typically correspond to protein segments within less ordered regions such as loops and turns. While the resolution of HXMS experiments does not allow precise identification of specific loops, 5 min exchange data indicate that some of these short loops/turns are located within residues 119–126, 133–148 and 182–196. The presence of such structures is also evident within the 81–118 region.

While very strong protection against H/D exchange as observed for $PrP^{Sc}$ is typically a hallmark of intermolecular ß-structure (especially in amyloid fibrils), in principle, slow exchange could also be associated with hydrophobic α-helices that are shielded from water as a result of burial in an apolar protein interior. However, native α-helices in $PrP^{C}$ are relatively polar and largely solvent-exposed. Consistent with this polar nature, for the vast majority of peptic fragments derived from native α-helices in $PrP^{C}$ there is essentially complete exchange of amide protons within 2 hours[12]. This contrasts sharply with little deuterium labeling observed for the same peptic fragments in $PrP^{Sc}$ (even after 240 hours of exchange), arguing against the possibility that any native $PrP^{C}$α-helices are preserved upon conversion to $PrP^{Sc}$. Aggregation alone is highly unlikely to limit solvent accessibility to a degree that could account for amide hydrogen exchange protection observed in the present study. Indeed, even when very tightly packed by centrifugation, amyloid fibrils formed by the recombinant PrP (rPrP) show high degree of protection only in the region corresponding to the ß-sheet core[12,14], and non-specific rPrP aggregates formed at elevated temperature display little long-term protection against deuterium incorporation (Supplementary Fig. 2). Furthermore, electron micrographs of $GPI^{-}PrP^{Sc}$ preparations reveal that they consist of amyloid fibrils that are relatively loosely packed, with abundant surface area exposed to solvent (Supplementary Fig. 3). Strong evidence for this in the electron micrographs comes from the stained surfaces themselves, which correspond to areas penetrated by the high molecular mass stain used, methylamine tungstate (~400 Da). Thus, the present HXMS data strongly suggest that the $PrP^{C}\rightarrow PrP^{Sc}$ conversion involves major refolding of the entire region C-terminal to residue ~80–90, and that the PK-resistant domain of $PrP^{Sc}$ consists of a network of ß-strands and relatively short connecting turns/loops, with no native α-helices present.

The model for $PrP^{Sc}$ structure most frequently discussed in the literature postulates that residues within the 89–175 segment form left-handed ß-helices (with a long unstructured loop encompassing residues 145–163), whereas the C-terminal region retains the native-like α-helical conformation of $PrP^{C}$ (refs. 15,16). An alternative 'spiral' model, based on molecular dynamics simulations, proposes that the ß-structure core of $PrP^{Sc}$ protofibrils is composed of a small, three short stranded ß-sheet (residues 116–119, 129–132, and 160–164), and an isolated strand 135–140, with all three α-helices retaining their native conformation[17]. The notion that the PK-resistant domain of $PrP^{Sc}$ retains some (or all) native α-helices is based on the interpretation of infrared spectra[8,10,18] and, especially, the presence of the ~1656–1660 $cm^{-1}$ band[8,18], the assignment of which is somewhat uncertain (see Supplementary Discussion). By contrast, circular dichroism data argue against the presence of any α-helices in $PrP^{Sc}$ (ref. 9). To further probe this issue, we examined the infrared spectrum of $GPI^{-}$ $PrP^{Sc}$ and compared it directly (i.e. using the same instrument and sampling method) with that of rPrP amyloid fibrils which are known to form parallel ß-structure, with no α-helices present[12,14]. While the spectra for the two samples show some differences in low-frequency bands representing ß-structure, both of them display essentially identical bands at 1660 $cm^{-1}$ (Supplementary Fig. 4). Since rPrP amyloid fibrils contain no αhelices, we conclude that the 1660 $cm^{-1}$ band cannot be considered as evidence for α-helical structure in brain-derived $PrP^{Sc}$.

Clearly, none of the models for $PrP^{Sc}$ structure proposed in the literature is compatible with the present experimental data, since these data show a particularly high degree of protection against H/D exchange for the regions predicted to form unstructured loops or native α-helices (Fig. 2). The general idea that $PrP^{Sc}$ structure is based on a ß-helical motif is not inconsistent with our HXMS data. However, such ß-helical structure would have to encompass essentially the entire PK-resistant region. Another, perhaps more likely possibility is that $PrP^{Sc}$ has a parallel, in-register ß-structure, a motif observed in many amyloids[19]. The propensity of PrP amino acid sequence to form parallel in-register ß-structure is indicated by studies with recombinant PrP amyloid fibrils[19] as well as crystallographic data for short peptide fragments[20].

The most intriguing aspect of TSE diseases is the phenomenon of prion strains that are associated with distinct disease phenotypes. While it is believed that these strain properties are encoded in distinct conformations of $PrP^{Sc}$ (refs. 1,2), the information regarding strain-specific $PrP^{Sc}$ conformational differences is very limited and difficult to interpret in terms of specific structural features. To bridge this gap, we extended our HXMS studies to $PrP^{Sc}$ corresponding to other strains of mouse scrapie, Chandler and ME7. Akin to $GPI^{-}$22L $PrP^{Sc}$, the entire PK-resistant cores of $GPI^{-}$ Chandler and ME7 $PrP^{Sc}$ are characterized by very high degree of protection against deuterium labeling (Fig. 1c–d). However, this protected core region in ME7 $PrP^{Sc}$ is eight residues longer compared to 22L and Chandler strains. Furthermore, for most peptic fragments derived from the 127–223 region the degree of deuterium labeling is substantially larger for Chandler and ME7 than 22L (Fig. 3a–b), likely reflecting small differences (1–2 residues) in the length of some ß-strands (which appear to be longer within the ~127–223 region of 22L $PrP^{Sc}$) and loops between them. Region-specific differences in the degree of deuterium labeling can also be detected between Chandler and ME7 $PrP^{Sc}$ (Fig. 3c). The finding that strain properties may be encoded not

only by differences in the length of the ordered ß-core region but also by relatively minor differences in the identity of internal ß-strands is consistent with an arrangement such as a parallel in-register ß-structure, as in this type of structure strands within the middle part of the $PrP^{Sc}$ sequence could act as nucleation elements. By contrast, in a s-helical structure intermolecular contact sites responsible for nucleation would be limited to the ends of individual ß-helices. The pattern of deuterium labeling for all strains of brain-derived $PrP^{Sc}$ is quite different from that for amyloid fibrils formed spontaneously by the recombinant prion protein, in which case the exchange-protected ß-core region is much shorter, limited to residues ~160–220 (Fig. 1e and ref. 12). This fundamental difference may explain why the infectivity of fibrils formed by the recombinant PrP is very low.

## Supplementary Material

Refer to Web version on PubMed Central for supplementary material.

## Acknowledgments

This study was supported by NIH grants NS44158, NS38604 and AG14359, and by the Intramural Research Program of the National Institute of Allergy and Infectious Diseases.

## References

1. Prusiner SB. Proc Natl Acad Sci U S A. 1998; 95:13363–83. [PubMed: 9811807]
2. Cobb NJ, Surewicz WK. Biochemistry. 2009; 48:2574–85. [PubMed: 19239250]
3. Castilla J, Saa P, Hetz C, Soto C. Cell. 2005; 121:195–206. [PubMed: 15851027]
4. Deleault NR, Harris BT, Rees JR, Supattapone S. Proc Natl Acad Sci U S A. 2007; 104:9741–6. [PubMed: 17535913]
5. Kim JI, et al. J Biol Chem. 2010; 285:14083–7. [PubMed: 20304915]
6. Wang F, Wang X, Yuan CG, Ma J. Science. 327:1132–5. [PubMed: 20110469]
7. Wuthrich K, Riek R. Adv Protein Chem. 2001; 57:55–82. [PubMed: 11447697]
8. Caughey BW, et al. Biochemistry. 1991; 30:7672–80. [PubMed: 1678278]
9. Safar J, Roller PP, Gajdusek DC, Gibbs CJ Jr. Protein Sci. 1993; 2:2206–16. [PubMed: 7905316]
10. Gasset M, Baldwin MA, Fletterick RJ, Prusiner SB. Proc Natl Acad Sci U S A. 1993; 90:1–5. [PubMed: 8419912]
11. Toyama BH, Kelly MJ, Gross JD, Weissman JS. Nature. 2007; 449:233–7. [PubMed: 17767153]
12. Lu X, Wintrode PL, Surewicz WK. Proc Natl Acad Sci U S A. 2007; 104:1510–5. [PubMed: 17242357]
13. Chesebro B, et al. Science. 2005; 308:1435–9. [PubMed: 15933194]
14. Cobb NJ, Sonnichsen FD, McHaourab H, Surewicz WK. Proc Natl Acad Sci U S A. 2007; 104:18946–51. [PubMed: 18025469]
15. Govaerts C, Wille H, Prusiner SB, Cohen FE. Proc Natl Acad Sci U S A. 2004; 101:8342–7. [PubMed: 15155909]
16. Wille H, et al. Proc Natl Acad Sci U S A. 2009; 106:16990–5. [PubMed: 19805070]
17. DeMarco ML, Daggett V. Proc Natl Acad Sci U S A. 2004; 101:2293–8. [PubMed: 14983003]
18. Spassov S, Beekes M, Naumann D. Biochim Biophys Acta. 2006; 1760:1138–49. [PubMed: 16730908]
19. Wickner RB, Shewmaker F, Kryndushkin D, Edskes HK. Bioessays. 2008; 30:955–64. [PubMed: 18798523]
20. Sawaya MR, et al. Nature. 2007; 447:453–7. [PubMed: 17468747]

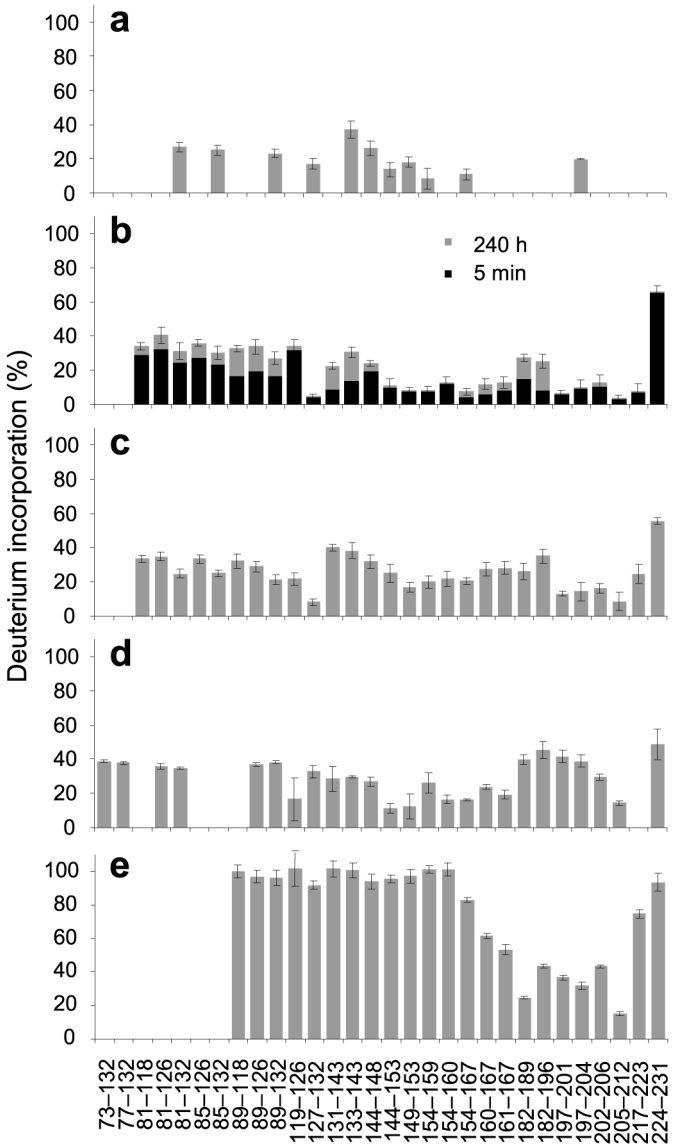


**Figure 1.**

Deuterium incorporation for peptic fragments derived from different types of misfolded prion protein aggregates. (**a**) $PrP^{Sc}$ from wild-type mice infected with 22L strain of scrapie after 240 hours of exchange. (**b**) $PrP^{Sc}$ from transgenic $GPI^{-}$ mice infected with 22L strain of scrapie after 5 min and 240 hours of exchange. (**c**) $PrP^{Sc}$ from transgenic $GPI^{-}$ mice infected with Chandler strain of scrapie after 240 hours of exchange. (**d**) $PrP^{Sc}$ from transgenic $GPI^{-}$ mice infected with ME7 strain of scrapie after 240 hours of exchange. (**e**) Amyloid fibrils formed from the recombinant mouse prion protein 89–231 after 240 h of exchange. Error bars indicate s.d.

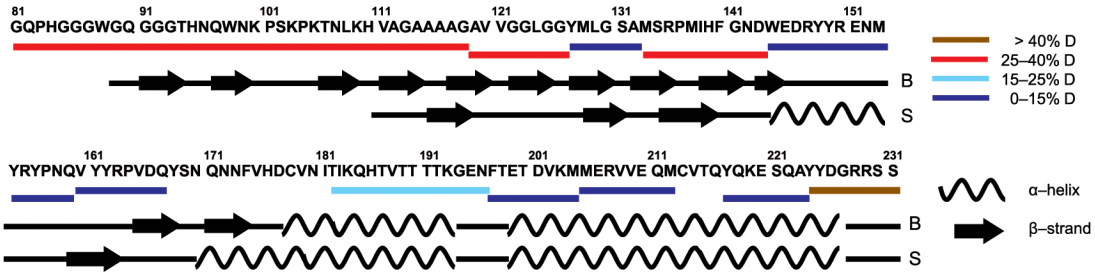


**Figure 2.**

Schematic representation of prion protein secondary structure in the ß-helix (B) and spiral (S) models of $PrP^{Sc}$. Black arrows, curved lines and solid lines represent ß-strands,α-helices and loops/unordered segments, respectively. Colour bars immediately below the sequence represent the percentage of deuterium incorporation for $GPI^{-}22L$ $PrP^{Sc}$ after 240 hours of exchange.

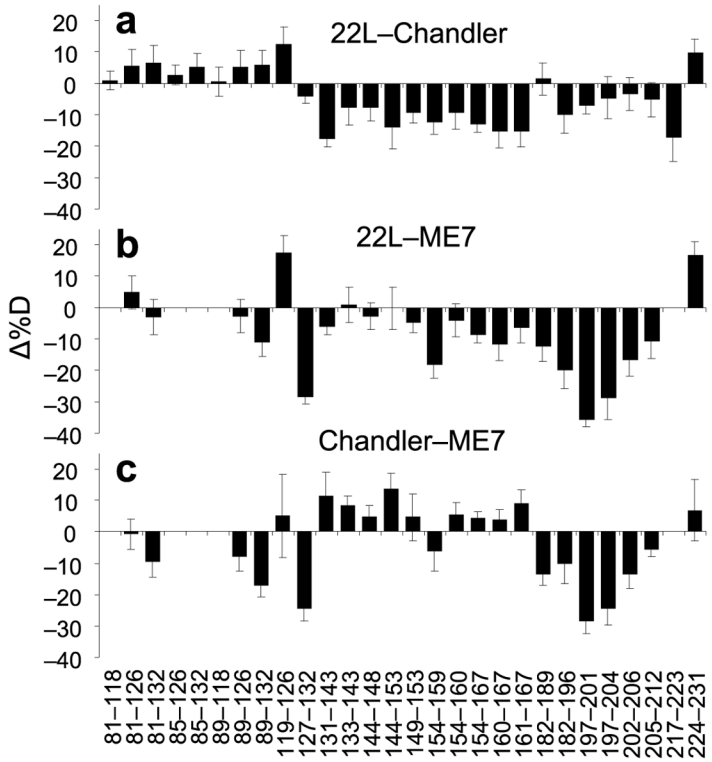


**Figure 3.**

Pairwise comparison of difference in deuterium labeling after 240 h exchange for different $PrP^{Sc}$ strains. (**a**) 22L and Chandler GPI $PrP^{Sc}$. (**b**) 22L and ME7 $GPI^{-}PrP^{Sc}$. (**c**) Chandler and ME7 $GPI^{-}PrP^{Sc}$. Data are based on 3–5 experiments using two different preparations of 22L and Chandler $GPI^{-}PrP^{Sc}$ and a single preparation of ME7 $GPI^{-}PrP^{Sc}$. Error bars indicate s.d.